

The Effect of Hydroxylamine on the Activity and Aggregate Structure of Autotrophic Nitrifying Bioreactor Cultures

Willie F. Harper Jr.,^{1,2} Akihiko Terada,³ Franck Poly,⁴ Xavier Le Roux,⁴ Ken Kristensen,³ Mustafa Mazher,⁵ Barth F. Smets³

¹Department of Civil and Environmental Engineering, University of Pittsburgh, Pittsburgh, Pennsylvania 15260; telephone: 412-624-9548; fax: 412-624-0135; e-mail: wharper@pitt.edu

²Department of Bioengineering, University of Pittsburgh, Pittsburgh, Pennsylvania 15260

³Department of Environmental Engineering, Technical University of Denmark, Lyngby, Denmark

⁴UMR 5557, Ecologie Microbienne Villeurbanne, CNRS, Université Lyon 1, USC INRA 1193, Lyon, France

⁵Department of Biological Sciences, Auburn University, Auburn, Alabama

Received 29 June 2008; revision received 4 September 2008; accepted 5 September 2008

Published online 17 September 2008 in Wiley InterScience (www.interscience.wiley.com). DOI 10.1002/bit.22121

ABSTRACT: Addition of hydroxylamine (NH₂OH) to autotrophic biomass in nitrifying bioreactors affected the activity, physical structure, and microbial ecology of nitrifying aggregates. When NH₂OH is added to nitrifying cultures in 6-h batch experiments, the initial NH₃-N uptake rates were physiologically accelerated by a factor of 1.4–13. NH₂OH addition caused a 20–40% decrease in the median aggregate size, broadened the shape of the aggregate size distribution by up to 230%, and caused some of the microcolonies to appear slightly more dispersed. Longer term NH₂OH addition in fed batch bioreactors decreased the median aggregate size, broadened the aggregate size distribution, and decreased NH₃-N removal from >90% to values ranging between 75% and 17%. This altered performance is explained by quantitative fluorescence in situ hybridization (FISH) results that show inhibition of nitrifying populations, and by qPCR results showing that the copy numbers of *amoA* and *nxrA* genes gradually decreased by up to an order-of-magnitude. Longer term NH₂OH addition damaged the active biomass. This research clarifies the effect of NH₂OH on nitrification and demonstrates the need to incorporate NH₂OH-related dynamics of the nitrifying biomass into mathematical models, accounting for both ecophysiological and structural responses.

Biotechnol. Bioeng. 2009;102: 714–724.

© 2008 Wiley Periodicals, Inc.

KEYWORDS: nitrification; hydroxylamine; aggregate size; microcolony; ammonia oxidizers; nitrite oxidizers

Introduction

Nitrification is a critical biochemical process needed as part of most modern municipal water pollution control facilities. Ammonia must be removed from wastewater in order to prevent eutrophication of receiving waters, and regulatory agencies in Europe and the United States have responded to this need by promulgating very strict (e.g., <0.5 mg N/L) effluent NH₃-N limits. The water quality community must therefore continue to improve the control of existing biological nitrogen removal facilities, to understand sources of disfunctioning of these facilities, and also to develop new novel technologies that improve performance and reduce costs. Improving our understanding of the underlying biochemical features of nitrification is essential to achieve these engineering goals.

Ammonia-oxidizing bacteria (AOB) use a well-known two-step process catalyzed by ammonia monooxygenase (AMO) and hydroxylamine oxidoreductase (HAO). AMO catalyzes the oxidation of NH₃-N to hydroxylamine (NH₂OH) and HAO catalyzes the oxidation of NH₂OH to NO₂⁻. Although NH₂OH is a biodegradable intermediate, it may accumulate in nitrifying cultures (Blackburne et al., 2003; Dua et al., 1979; Schmidt et al., 2004; Yang and Alleman, 1992). It has been suggested that NH₂OH inhibits ammonia oxidation (Blackburne et al., 2003; Hyman and Wood, 1983; Yang and Alleman, 1992). For example, Yang and Alleman (1992) suggested that free NH₂OH inhibits nitrogen removal in simultaneous nitrification and denitrification systems. Some evidence also suggests that NH₂OH can enhance nitrification. For example, de Bruijn et al.

Correspondence to: W.F. Harper Jr.

Additional Supporting Information may be found in the online version of this article.

(1995) added NH_2OH to ammonia-limited chemostats, gradually increasing the NH_2OH concentration from 1.4 to 10.4 mM, and they found that the overall biomass yield increased as they increased the influent NH_2OH load. Böttcher and Koops (1994) observed growth of *Nitrosomonas europaea*, *Nitrosomonas nitrosa*, and *Nitrosococcus oceanus* on ammonia supplemented with relatively small amounts of NH_2OH , and reported that molar yields and oxygen consumption were greater with NH_2OH than without it. This demonstrates that NH_2OH enhances nitrification, but it is not clear how these findings can be reconciled with the results that describe NH_2OH as a nitrification inhibitor.

Kuai and Verstraete (1998) anaerobically incubated NH_2OH with sludge taken from an oxygen-limited autotrophic nitrification–denitrification bioreactor. They found that the NH_2OH -amended sludge simultaneously removed $\text{NH}_3\text{-N}$ and $\text{NO}_2^- \text{N}$ at a rate that was six times greater than that of the control (no NH_2OH); these results suggest that NH_2OH accelerated ammonia removal, but the mechanism responsible for this remains unclear. Kindaichi et al. (2004a) also reported that the oxidation of $\text{NH}_3\text{-N}$ was stimulated by NH_2OH addition in their study of nitrifying biofilms. They also studied the growth pattern of *Nitrosomonas* species using fluorescent hybridization probes, and they found that the addition of NH_2OH changed the growth pattern from dense to more loosely arranged cell microcolonies. They were also unable to identify nitrite-oxidizing bacteria (NOB) in the NH_2OH -treated biofilms, which suggested that NH_2OH may also select against NOBs (as a side-effect).

There are two possible explanations for NH_2OH -induced acceleration of NH_3 removal rates. First, HAO (located in the periplasm) may oxidize NH_2OH and then channel electrons back to AMO (located in the transmembrane space) via cytochrome-554 and ubiquinone 8 (Watson et al., 1984); this in turn may provide the reducing equivalents required to allow AMO to function at maximum capacity. Such NH_2OH -mediated acceleration of NH_3 oxidation was recently well-documented in batch nitrifying cultures by Chandran and Smets (2008). The second hypothesis is that NH_2OH may cause floc disaggregation, leading to enhanced ammonia oxidation because of reduced mass transfer limitations. This idea is suggested by the results of Kindaichi et al. (2004a) who found that NH_2OH addition dispersed AOB microcolonies. Testing this hypothesis means determining whether NH_2OH -induced dispersal can shift the size distribution of planktonic aggregates. The overall objectives of the current study are to (1) investigate the two hypotheses related to NH_2OH -induced acceleration of NH_3 removal rates, and (2) reconcile the apparently conflicting reports that describe NH_2OH as either an enhancer or inhibitor of nitrification. In order to pursue these objectives, the short and longer term effects of NH_2OH addition was determined over a range of NH_2OH concentrations, and the nitrifying biomass was analyzed to assess metabolic activity, aggregate size

distribution, microcolony structure, and the nitrifier (AOB and NOB) population levels.

Materials and Methods

Experimental Overview

Two types of systems were operated, one continuous-flow nitrifying bioreactor (NBR) and eight fed-batch bioreactors (FBBRs). Biomass from the NBR was used to test the effect of NH_2OH in short term (6-h) batch tests. Longer term effects (several days) were tested by using the FBBRs. Samples were analyzed for $\text{NH}_3\text{-N}$, aggregate size distribution, and FISH/confocal microscopy analysis. Samples taken from the FBBRs were also analyzed for AOB and NOB abundance by quantitative fluorescence in situ hybridization (FISH), and for *amoA* and *nxrA* gene abundance by quantitative PCR (qPCR).

Continuous Flow Nitrifying Bioreactor (NBR)

The NBR consisted of a 10 L plastic mixing vessel and 2.6 L settler. The air needed for nitrification and for mixing was supplied by an air pump through an air diffuser. The hydraulic residence time was 1 day and the solids retention time was 20 days. The pH was maintained at 7.3 by a pH controller. The influent $\text{NH}_3\text{-N}$ concentration was 300 mg N/L, and the feed also consisted of (in mg/L): $\text{MgSO}_4 \cdot 7\text{H}_2\text{O}$ (280), $\text{K}_2\text{H}_2\text{PO}_4$ (27), $\text{CaCl}_2 \cdot 2\text{H}_2\text{O}$ (120), NaCl (600), $\text{FeSO}_4 \cdot 7\text{H}_2\text{O}$ (3.3), $\text{MnSO}_4 \cdot \text{H}_2\text{O}$ (3.3), $\text{CuCl}_2 \cdot 2\text{H}_2\text{O}$ (0.8), $\text{ZnSO}_4 \cdot 7\text{H}_2\text{O}$ (1.7), and $\text{NiSO}_4 \cdot 6\text{H}_2\text{O}$ (0.3). The sludge concentration was typically 700 mg TSS/L. Prior to use in these experiments, the reactor had been operated for several months under steady state conditions, with typical effluent concentrations 1 mg/L $\text{NH}_3\text{-N}$, 280 mg/L $\text{NO}_3^- \text{N}$, and 0.4 mg/L $\text{NO}_2^- \text{N}$.

Batch Tests

Biomass (250 mL) was harvested from the NBR, washed twice, and re-suspended in each of two 500 mL volumetric flasks. The working volume was 250 mL, and the media was the same as the NBR feed. The flasks were oxygenated with an air pump and were pH buffered (between pH 7.5 and 8.0) with sodium bicarbonate. Ammonia was added to both flasks at an initial concentration of 150 mg N/L, and NH_2OH was added to one flask at an initial concentration of 15 mg N/L. Sampling was conducted over the course of 6 h to determine $\text{NH}_3\text{-N}$ and NH_2OH , and biomass samples were taken at the beginning and at end of the batch test for aggregate size analysis and for FISH/confocal imaging. This test was repeated four times, and each test was labeled test A, B, C, and D respectively. Initial $\text{NH}_3\text{-N}$ uptake rates were determined using data collected over the first 110 min of the batch test.

Fed-Batch Bioreactors (FBBRs)

Eight replicate FBBRs were initiated with biomass from the NBR. Initial biomass concentrations were approximately 500 mg/L TSS, and all reactors were batch-fed with ammonia at 200 mg NH₄⁺-N/L. The FBBRs were monitored for pH and aerated. After complete removal of ammonia (2 days), aeration was halted, biomass removed (to retain a target SRT of 10 days), the bioreactors spiked with fresh media, and the cycle repeated. At the beginning of each operating day, evaporative losses (typically 2–5% of the FBBR working volume) were measured and corrected by adding DI water. The flasks were operated for 57 days (28 cycles). On day 58, NH₂OH was added at different doses for an additional 21 days. The NH₂OH-N/L target concentrations were 40 mg NH₂OH-N/L (FBBR7 and FBBR8), 20 mg NH₂OH-N/L (FBBR5 and FBBR6), 10 mg NH₂OH-N/L (FBBR3 and FBBR4), and 0 mg NH₂OH-N/L (FBBR1 and FBBR2). These concentrations were selected so that the range of molar ratios of NH₄⁺-N/NH₂OH-N overlaps with the molar ratio used by Kindaichi et al. (2004a) (they used a molar ratio of 14.4).

Abiotic Control Experiments

Two types of abiotic control experiments were conducted in sterilized NBR media. Each test was done in a sealed 250 mL volumetric flask for 6 h at pH = 7.5 and *T* = 23°C, and no oxygen was provided. First, NH₂OH (at 10, 20, and 40 mg/L) was gently mixed with NH₄Cl (at 200 mg N/L). Second, NH₂OH (at 10, 20, and 40 mg/L) was mixed with FeSO₄·7H₂O (at 0.7 mg/L as Fe²⁺). As expected, the NH₂OH concentration did not change during any of these experiments (data not shown).

Analytical Methods

NH₃-N, NO₂⁻-N, and NO₃⁻-N concentrations were determined spectrometrically with Spectroquant kits (Merck, Darmstadt, Germany) using methods analogous to Standard Methods (4500-NH₃, 4500-NO₂, 4500-NO₃) (APHA, 1992). NH₂OH was determined colorimetrically as described in

Frear and Burrell (1955), except that the phosphate solution was buffered at pH 7.0. Total and volatile suspended solids were determined as described in Standard Methods (2540-solids) (APHA, 1992).

Aggregate Size Analysis

Aggregate size distributions were determined using a Malvern Mastersizer 2000 (Worcestershire, United Kingdom) Laser Particle Sizer with an operating range of 0.05–900 μm and an active beam length of 2.4 mm. The detector alignment was done before the beginning of each analysis session, and background measurement was done prior to each measurement.

Fluorescence In Situ Hybridization (FISH)

Biomass samples were fixed in 4% paraformaldehyde solution for 3 h at 4°C. Then, the fixed samples were washed with 1× phosphate-buffered saline (PBS) three times to remove residual paraformaldehyde and stored in PBS/ethanol (1:1) at –20°C. About 8 μL of the sample was applied to each well on a gelatine-coated glass slide and the slide was dried for 15 min at 46°C and dipped into 50%, 80%, and 96% (v/v) ethanol for 3 min each to dehydrate the samples. FISH was conducted according to the protocol by Amann (1995). The applied oligonucleotide probes are shown in Table I. The probes were labeled at the 5' end with 5(6)-carboxyfluorescein-N-hydroxysuccinimide ester (FLUOS) and indocarbocyanine dye Cy3. Non-EUB probes, which are labeled with FLUOS and Cy3, were also applied to check for cellular autofluorescence and unspecific adhesion of probes or fluorochromes. The samples were observed by confocal laser scanning microscopy (CLSM) (TCS SP5, Leica, Germany) with an Ar laser (488 nm) and HeNe laser (543 nm). Optical sectioning was performed to obtain stacks, which were used to carry out 3D reconstruction of the image. Three z-stacks (stepsize: 0.5 μm) were captured from each biomass sample and exported as series of TIFF files. Quantification, based on a biovolume fraction (specific AOB or NOB probe-conferred area to EUBmix-conferred

Table I. FISH oligonucleotide probes used in this study.

Probe	OND designation ^a	Target	Probe sequence (5'–3')	FA (%)	References
EUB338	S-D-Bact-0338-a-A-18	Most bacteria	GCT GCC TCC CGT AGG AGT	0–40	Amann et al. (1990)
EUB338 II	S-*-BactP-0338-a-A-18	<i>Planctomycetales</i>	GCA GCC ACC CGT AGG TGT	0–40	Daims et al. (1999)
EUB338 III	S-*-BactV-0338-a-A-18	<i>Verrucomicrobiles</i>	GCT GCC ACC CGT AGG TGT	0–40	Daims et al. (1999)
Non-EUB	S-*-Bact-338-a-B-18	Comp EUB	ACT CCT ACG GGA GGC AGC	0–40	Wallner et al. (1993)
NSO190	S-F-bAOB-0189-a-A-19	Most beta-AOB	CGA TCC CCT GCT TTT CTC C	35 ^b	Mobarry et al. (1996)
NIT3 ^c	S-G-Nbac-1035-a-A-18	<i>Nitrobacter</i> spp	CCT GTG CTC CAT GCT CCG	40	Wagner et al. (1996)
Ntspa662 ^c	S-G-Ntspa-662-a-A-18	Genus <i>Nitrospira</i>	GGA ATT CCG CGC TCC TCT	35	Daims et al. (2001)

^aAlm et al. (1996).

^bPynaert et al. (2003).

^cUnlabeled competitor for each probe (same concentration) was used as indicated in the reference.

area), was performed after intensity thresholding and noise reduction by using Daime (Daims et al., 2006).

Preparation of Ammonia Monooxygenase (*amoA*)-Containing Plasmids Used for Quantification of *amoA* Genes

An *amoA* standard was prepared by amplifying DNA extracted from *N. europaea* (ATCC19178) (Iizumi et al., 1998) with forward and reverse primer of *amoA* 1f (5'-GGG GTT TCT ACT GGT GGT-3') and 2r (5'-CCC CTC KGS AAA GCC TTC TTC-3') (Rotthauwe et al., 1997). The amplified fragment (length: 491 bp) was extracted and cleaned by QIAEX II (Qiagen, Inc., Valencia, CA) and subsequently ligated with a pCR[®]2.1-TOPO[®] vector (Invitrogen, Carlsbad, CA). The vector plasmid was inserted into One Shot[®] TOP10 Chemically competent *E. coli* (Invitrogen). Plasmid DNA was extracted by QIAprep[®] Miniprep (Qiagen), quantified by a spectrophotometer at 260 nm, and diluted to attain standard solutions with copy numbers from 1.0×10^8 to 1.0×10^1 per 5 μ L. There was a high correlation between log *amoA* copy number and cycle number ($r^2 = 0.9X$), and the result was reproducible. The detection limit was 10^3 copies/ng-DNA.

Preparation of Nitrite Oxidoreductase (*nxrA*)-Containing Plasmids Used for Quantification of *nxrA* Genes

A *nxrA* standard derived from *Nitrobacter hamburgensis* (Poly et al., 2008) and standard solutions from 1.0×10^8 to 1.0×10^1 per 5 μ L were prepared. Forward and reverse primers F1norA (5'-CAG ACC GAC GTG TGC GAA AG-3') (Poly et al., 2008) and R2norA (5'-TCC ACA AGG AAC GGA AGG TC-3') (Wertz et al., 2008) amplified a 322 bp fragment. The detection limit was 50 copies/ng-DNA.

DNA Extraction and RT-qPCR for *amoA* and *nxrA* Quantification

Biomass samples (2 mL) were taken from each FBBR and the DNAs were extracted with a Fast DNA spin kit (Bio101, Qbiogene, Inc., Carlsbad, CA) by following the manufacturer's instructions. Concentrations of the DNA were measured at a wavelength of 260 nm by a spectrophotometer (Cary 50, VARIAN, Walnut Creek, CA). RT-qPCR for *amoA* was performed in a volume of 25 μ L, which contains 12.5 μ L of mixture of SYBR green PCR master mix (iQTM SYBR[®] Green Supermix; Bio-Rad, Hercules, CA), 0.5 μ L of each primer (20 μ M), 6.5 μ L of molecular grade H₂O and 5 μ L of template solution adjusted at 2 ng-DNA/ μ L. Thermal conditions for *amoA* were initiated by pre-heating at 94°C for 5 min, followed by 45 cycles of 94°C for 1 min, 56°C for 30 s, 72°C for 30 s, and 80°C for 1 s (acquisition data step). All procedures including PCR and data analysis were performed by Chromo4TM System (Bio-Rad). All samples,

including control reactions without template DNAs were measured in triplicates. RTqPCR for *nxrA* was performed in a volume of 20 μ L, which contains 10 μ L of mixture of SYBR green PCR master mix (MIX Qiagen, Inc.), 1 μ L of each primer (10 μ M), 3 μ L of molecular grade H₂O and 5 μ L of template solution adjusted at 2 ng-DNA/ μ L. Thermal conditions for *nxrA* were initiated by pre-heating at 95°C for 15 min, followed by 45 cycles of 95°C for 30 s, 55°C for 45 s, and 72°C for 45 s. All procedures including PCR and data analysis were performed by LightCycler[®] 480 (Roche Diagnostics, Meylan, France). All samples, including control reactions without template DNA, were measured in triplicate.

Results

The Short Term Effects of NH₂OH Addition

The short term effects of NH₂OH addition were investigated using batch tests with nitrifying biomass (Fig. 1). Complete removal of NH₃-N was observed in each batch test, but when NH₂OH was present the initial NH₃-N removal rates were 1.4–13 times higher. Most of the measured initial NH₃-N removal rates were between 3.1 and 8.3 g NH₃-N/g VSS/day, values that are consistent with the range of maximum specific NH₃-N removal rates determined previously (Rittmann and Snoeyink, 1984). The rate enhancement was most manifest for test B, where in absence of NH₂OH, NH₃ removal was almost non-detectable but matched other removal rates in the presence of NH₂OH. Figure 1 shows that NH₂OH was removed quickly, and the NH₃-N removal rate enhancement was only present when NH₂OH was also available. Therefore, the NH₃-N rate enhancement appears to be physiologically connected to the availability and bioprocessing of NH₂OH. This finding is consistent with the results recently documented by Chandran and Smets (2008).

NH₂OH addition changed the shape of the aggregate size distributions and caused the median aggregate size to decrease (Fig. 2). In test A, the median aggregate size decreased from 77 to 58 μ m, a 25% reduction. The d_{90}/d_{10} ratio, an index of the width of the size distribution, increased by 230% from 2.2 to 7.3. This shows that the size distribution broadened to increase the fraction of large and small aggregates. No such broadening occurred when NH₂OH was not added. Test B showed that the median aggregate size decreased by 36% from 143 to 91 μ m, and the d_{90}/d_{10} ratio increased by 113% from 4.6 to 9.8. These aggregate size shifts were not the reason for the increase in the initial NH₃-N removal rates because the rate enhancement was only present when NH₂OH was available. To the authors' knowledge, this result is the first to show that NH₂OH addition causes a shift in the aggregate size distribution of nitrifying biomass. This size shift effect stretches the distribution, resulting in a smaller median size.

Floc samples hybridized with NSO190-Cy3 and EUBmix probes-Fluo were used to explore the morphological effects of NH₂OH addition after the 6-h batch experiments (Fig. 3).

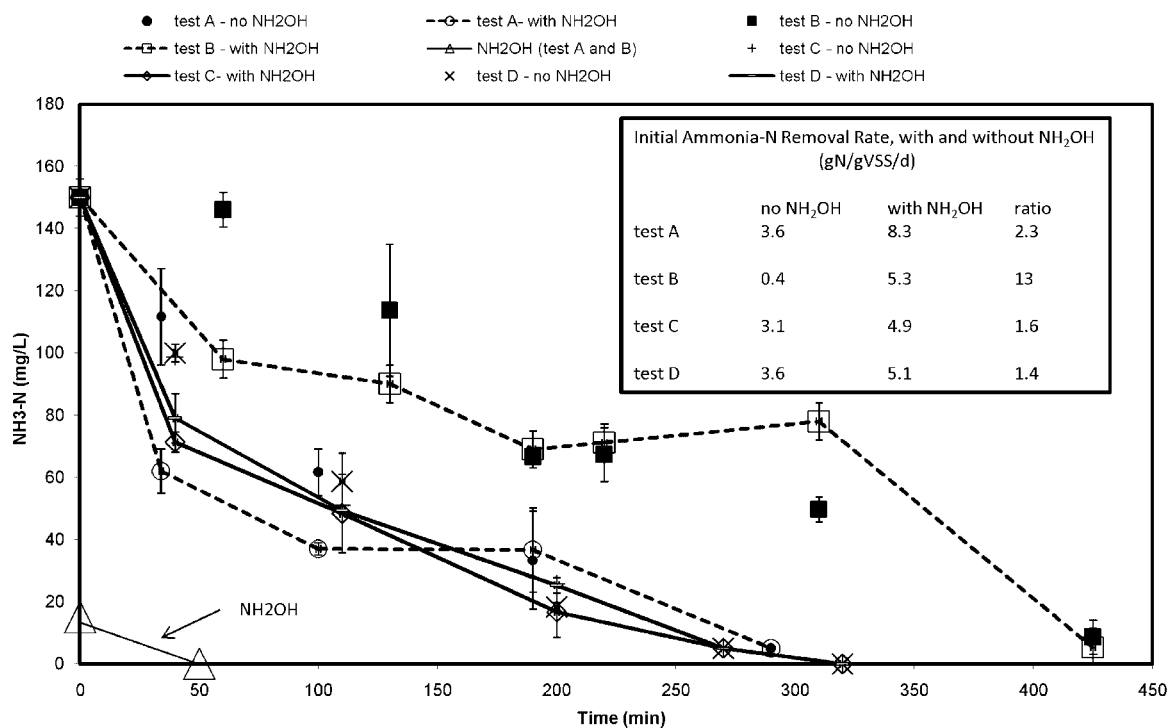


Figure 1. The effect of hydroxylamine on ammonia-N uptake: 6-h batch tests.

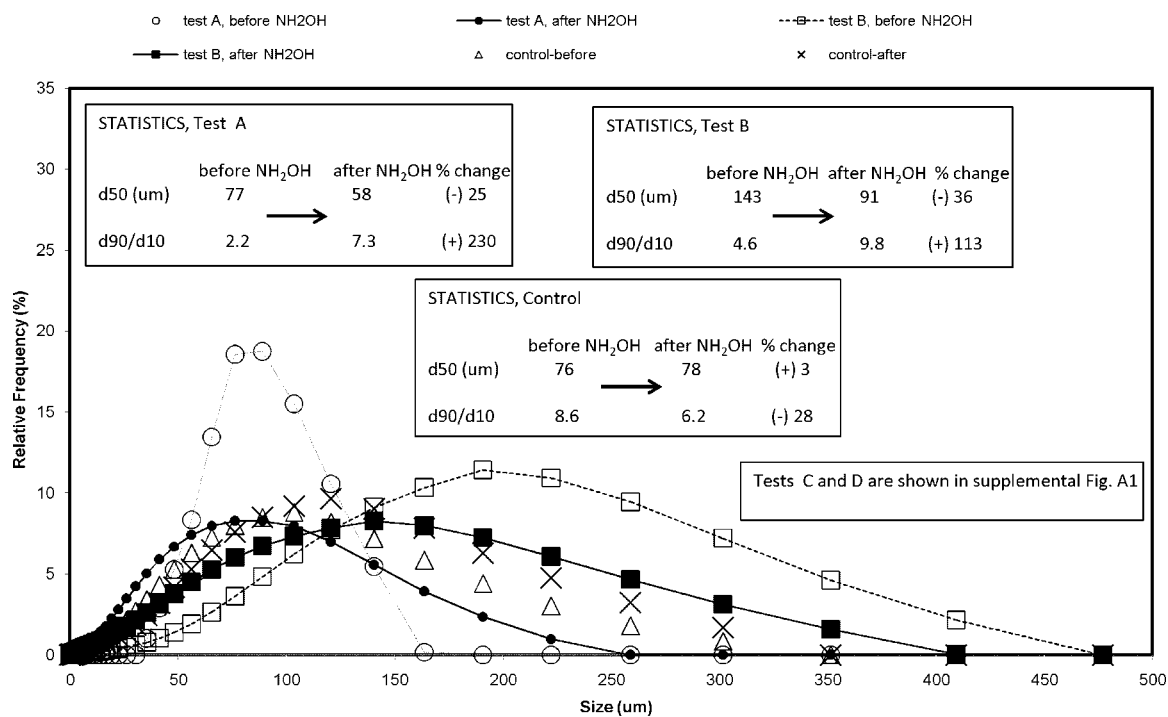


Figure 2. The effect of hydroxylamine on aggregate size distributions: 6-h batch tests.

Spherical microcolonies, approximately 5–10 μm in diameter, were visible, and they generally appeared tight and well-organized. These microstructures were visible before and after NH_2OH addition, but they were less numerous after NH_2OH addition, and single scattered cells became more common. This result is consistent with the observations of Kindaichi et al. (2004a). Before NH_2OH addition, the spherical clusters commonly aggregated to form larger structures, approximately 20–40 μm in diameter. These cluster aggregates were less numerous after NH_2OH addition. These results show that the microcolonies were more dispersed after NH_2OH addition.

The Longer Term Effects of NH_2OH Addition

FBBRs were used to explore the longer term effects of NH_2OH addition on nitrifying cultures. The FBBRs generally operated within a pH range of 7.5–8.8 and with TSS levels between 100 and 150 mg/L. Ammonia-N removal was typically 90% or greater prior to day 58, when NH_2OH addition commenced (Fig. 4). Initially, hydroxylamine addition did not affect the end-of-cycle ammonia-N levels, but on day 70, elevated ammonia-N levels were detected for all FBBRs receiving NH_2OH . The day 74 ammonia-N levels

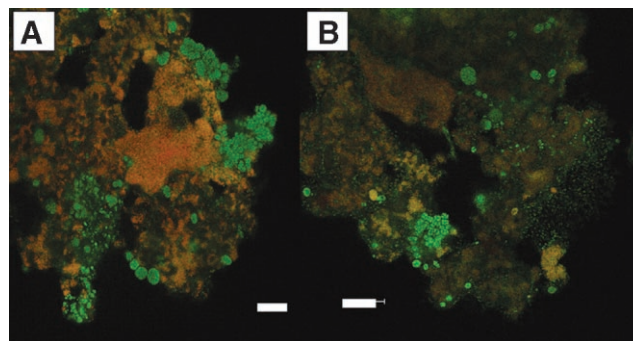


Figure 3. The effect of hydroxylamine on microcolony structure: 6-h batch tests. Floc samples hybridized with probes of NS0190-Cy3 and EUBmix-Fluo. NS0190- and EUBmix-conferred cells are shown in yellow and green, respectively: (A) NBR biomass from sample taken before the start of the 6-h incubation; (B) NBR biomass from sample taken after 6-h batch test with 15 mg N/L of NH_2OH .

ranged from 50 to 166 mg/L $\text{NH}_3\text{-N}$, which corresponds to a removal of 75–17%. The FBBRs that did not receive NH_2OH continued to remove >90% of the influent ammonia-N load. To the author's knowledge, these findings are the first

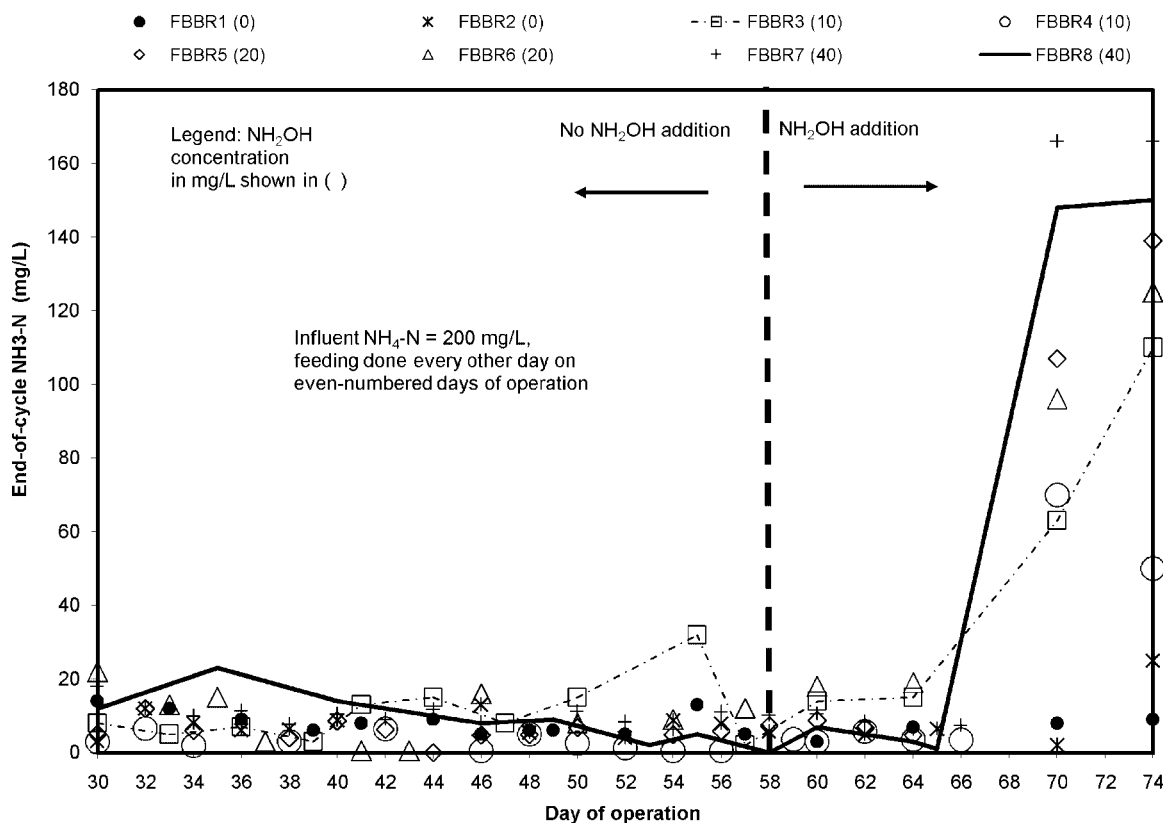


Figure 4. Fed-batch bioreactor performance before and after NH_2OH addition.

to show that longer term NH₂OH addition gradually causes poor performance in nitrifying cultures.

After NH₂OH addition, differences in the FBBR aggregate size distributions were observed. For example, the median aggregate size for FBBR6 (which was supplemented with 20 mg/L NH₂OH-N) shifted from 126 μm on day 57 (before NH₂OH addition) to 89 μm on day 64, and then to 48 μm on day 72 (see Appendix, Fig. A2). No such aggregate size shift was detected for FBBR2, which did not receive NH₂OH (see Appendix, Fig. A3). A two-tailed *T*-test was used to evaluate the statistical significance of the differences between median aggregate sizes (Table II). The *T*-test confidence levels were generally greater than 99%, even for the control (no NH₂OH) FBBRs, which shows that statistically significant aggregate size differences were present both with and without NH₂OH addition. This result was largely due to the precision associated with aggregate size determination. FBBR1 and FBBR2 did not receive NH₂OH and did not show the “broadening” of the aggregate size distribution. For FBBR1, the aggregate size distribution became narrower (e.g., d_{90}/d_{10} ratio decreased), and for FBBR2, the d_{90}/d_{10} ratio was constant. For the FBBRs receiving 10 and 20 mg/L NH₂OH (i.e., FBBR3 and FBBR4, and FBBR5 and FBBR6, respectively), the median aggregate size decreased and the d_{90}/d_{10} ratios increased, consistently with the size shifts observed in the aforementioned short term (batch) experiments. Addition of 40 mg/L NH₂OH did not immediately result in a size shift. The FBBR7 data showed that the aggregates were larger on day 64, and for FBBR8 very little change was observed from days 57 to 64. On day 72, the aggregate size shifted to a lower median size and a broader distribution in both cases. The relationship between the NH₂OH concentration and the observed effect was thus not linear.

Biomass taken from FBBRs and subjected to FISH probing is shown in Figure 5. Spherical clusters belonging to AOB (especially for *N. europaea*) were observed in the

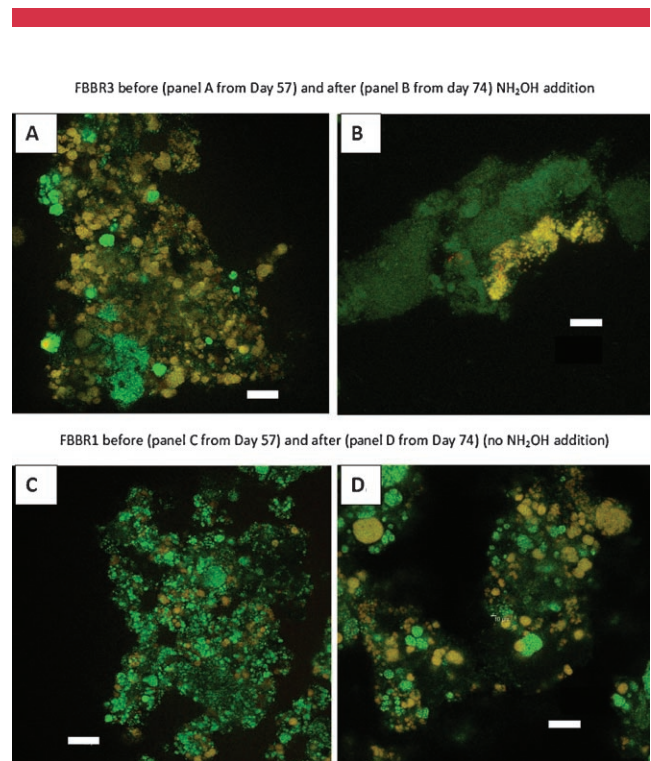


Figure 5. The effect of hydroxylamine on the microcolony structure in FBBR1 and FBBR3. Floc samples hybridized with probes of NS0190-Cy3 and EUBmix-Fluo (A and B). NS0190- and EUBmix-conferred cells are shown in yellow and green, respectively: (A) FBBR3 biomass from sample taken on day 57, before NH₂OH addition commenced on day 58; (B) FBBR3 biomass from sample taken on day 74, NH₂OH was added at 10 mg N/L; (C) FBBR1 biomass on day 57; (D) FBBR1 biomass on day 74. FBBR1 did not receive NH₂OH. Bars represent 20 μm (in panels A and C) or 10 μm (in panels B and D).

FBBRs without NH₂OH addition (Fig. 5, panels A, C, and D). Further investigations with other probes (Nsm156 and Nmo218) indicated that the spherical clusters (hybridizing only with EUB and thus appearing green in Fig. 5) belonged

Table II. FBBR aggregate size data and statistical comparison.

	FBBR1			FBBR2			FBBR3			FBBR4		
	Day 57	Day 64	Day 72	Day 57	Day 64	Day 72	Day 57	Day 64	Day 72	Day 57	Day 64	Day 72
Average size	78	73	50	87	82	107	60	65	49	107	91	66
Median size (d_{50})	65	56	44	75	65	88	54	47	38	89	75	48
^a Confidence (vs. day 57)	—	>99%	>99%	—	>99%	>99%	—	>99%	>99%	—	>99%	>99%
^b d_{90}/d_{10}	10.00	8.64	3.89	6.82	7.11	6.64	7.80	8.62	11.63	5.90	10.38	10.18
	FBBR5			FBBR6			FBBR7			FBBR8		
	Day 57	Day 64	Day 72	Day 57	Day 64	Day 72	Day 57	Day 64	Day 72	Day 57	Day 64	Day 72
Average size	154	97	55	152	73	52	72	92	55	107	110	65
Median size (d_{50})	134	80	46	126	89	41	57	73	42	87	92	49
Confidence (vs. Day 57)	—	>99%	>99%	—	>99%	>99%	—	>99%	>99%	—	>99%	>99%
d_{90}/d_{10}	2.90	8.45	8.64	7.56	8.93	9.60	7.29	7.45	7.69	8.68	6.55	8.13

^a% Confidence determined using the two-tailed *T*-test. This value refers to the comparison of median aggregate sizes.

^b d_{10} is the equivalent diameter where 10% of the aggregates have a smaller diameter. d_{90} is the equivalent diameter where 90% of the aggregates have a smaller diameter.

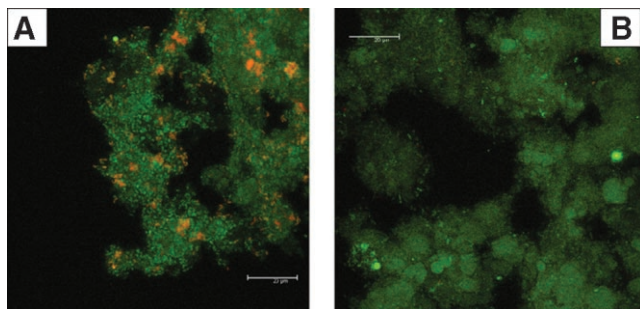


Figure 6. The effect of hydroxylamine on FISH images and the AOB/NOB populations. Fish images are hybridized with NSO190-Cy3, NIT3-Cy3 and EUBmix probes-Fluo. NSO190- and EUBmix-conferred cells are shown in yellow and green. **A:** Biomass in the reactor FBBR5 before hydroxylamine addition. **B:** Biomass in the reactor FBBR5 after hydroxylamine addition at 20 mg/L HA.

to *Nitrosomonas oligotropha* and *Nitrosococcus mobilis* (see Appendix, Fig. A4 for an example). NH_2OH addition dispersed the floc structure and reduced the visible abundance of AOB clusters (Fig. 5, panel B). The NH_2OH -exposed AOB microcolonies were approximately 4–8 μm in diameter, smaller than the 10–15 μm microcolonies observed before NH_2OH addition. This change in microstructure was not observed in FBBR1, which did not receive NH_2OH . Throughout the FBBR operations, *Nitrospira* spp. were not detected by Ntspa662 probe.

FISH analysis also provided insight into the effect of NH_2OH addition on the AOB versus NOB population levels (Fig. 6). Before NH_2OH addition, the NOB cells (shown in red as Nit3 positive cells) were scattered throughout the floc (Fig. 6, panel A). After NH_2OH addition, the Nit3 signals were fewer and more dispersed

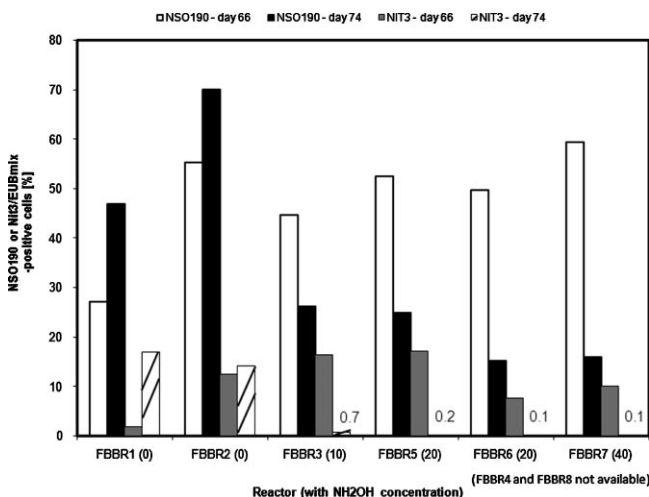


Figure 7. AOB and NOB percentages per all eubacteria on days 66 and 74.

(Fig. 6, panel B), suggesting that the NOB were inhibited by NH_2OH addition. Quantitative FISH analysis showed that NOB population levels were typically at 10–20% of total eubacteria abundance on day 66 (Fig. 7). On day 74, the NOB populations were below detection limit in all FBBRs receiving NH_2OH , which shows that NOB had been strongly inhibited. These findings were corroborated by end-of-cycle data showing that nitrite levels were <3 mg N/L on day 74 for FBBRs that did not receive NH_2OH , but for those receiving NH_2OH , the nitrite levels were higher and were between 9 mg N/L (FBBR4) and 24 mg N/L (FBBR3) on day 74. Figure 7 also shows that the AOB abundance declined from approximately 50% of total eubacteria on day 66 to 15–30% on day 74. Longer term NH_2OH addition gradually and negatively affected both AOB and NOB population levels. At day 66, the FBBR AOB and NOB relative abundances agreed well with population levels determined for the NBR (AOB: 47%; NOB: 13%). These data were also comparable to percentage abundances previously reported from biofilm studies. For example, Lydmark et al. (2006) found AOB and NOB percentage abundances of 20–45% and 30–40% respectively in a full-scale nitrifying trickling filter. Kindaichi et al. (2004b) found AOB and NOB percentage abundances of 22% and 28% respectively in a bench scale rotating disk bioreactor.

The *amoA* and *nxrA* gene levels were stable in the reactors that did not receive NH_2OH addition (FBBR1 and FBBR2), indicating that the reactors were stably operated (Fig. 8). For the FBBRs receiving 10 mg/L (FBBR3 and FBBR4) and 20 mg/L NH_2OH (FBBR5 and FBBR6), the *amoA* (Fig. 8, panel A) and *nxrA* (Fig. 8, panel B) copy numbers decreased gradually by up to an order of magnitude. Surprisingly, for the FBBRs receiving 40 mg/L NH_2OH , neither the *amoA* nor *nxrA* gene copy numbers declined on day 65, but these values dropped significantly on day 74. This shows that NH_2OH addition at 40 mg/L did not decrease the *amoA* copy numbers as quickly as what is observed at 10 and 20 mg/L. Longer term addition of NH_2OH decreased the abundance of *amoA* and *nxrA* genes, and these data agree well with the FBBR performance timeline (from Fig. 4). The dramatic decrease in *amoA* and *nxrA* gene abundances (day 74) mirrors the sharply elevated end-of-cycle ammonia-N levels measured on day 74. Addition of 20 mg/L of NH_2OH -N had the most critical impact on the *amoA* and *nxrA* gene pool (see Appendix, Fig. A5). The ratio of *amoA* to *nxrA* gene copy numbers for the control (no NH_2OH) FBBRs was close to 1, but for FBBRs receiving NH_2OH the ratio decreased to values less than 0.1. The lowest values were observed for FBBRs receiving 20 mg/L.

Discussion

There are two hypotheses that might explain why NH_2OH accelerates NH_3 -N uptake:

- (1) physiological stimulation via reducing equivalent supply to AMO, and

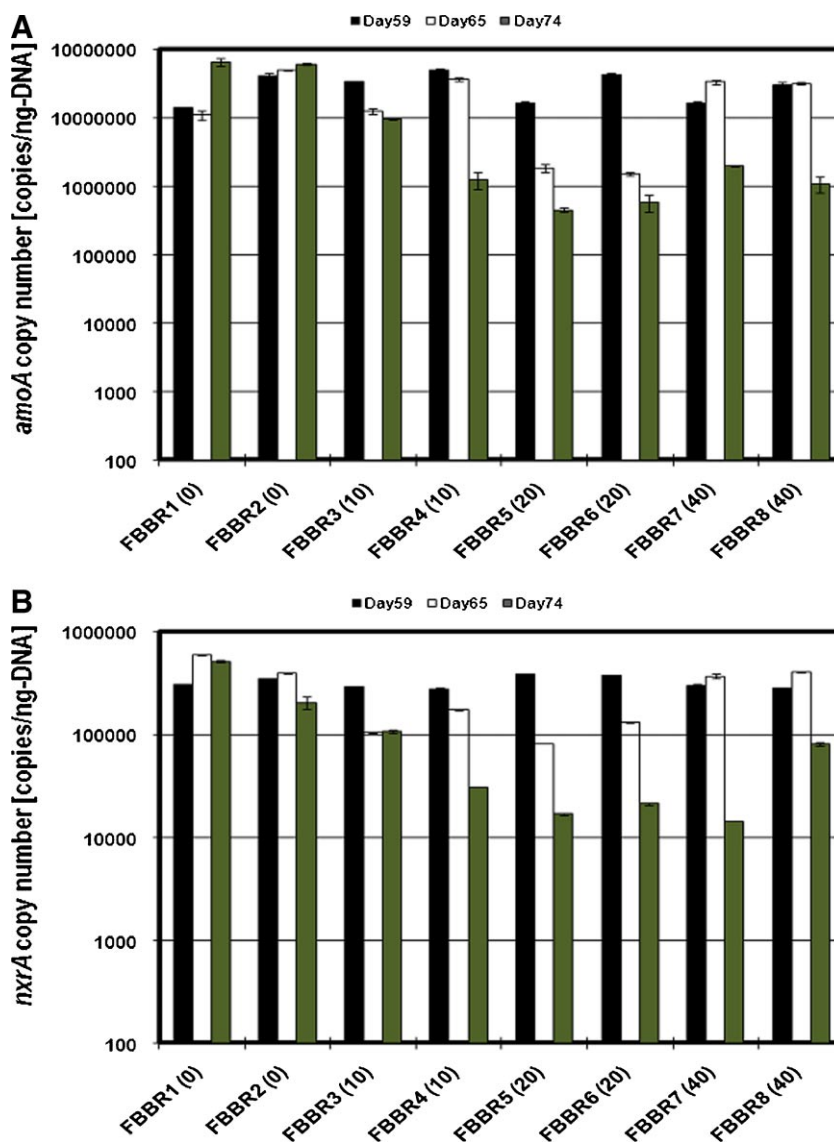


Figure 8. The effect of hydroxylamine on *amoA* gene (panel A) and *nxrA* gene (panel B) abundance. The horizontal axis shows the FBBRs and the corresponding hydroxylamine concentrations (in mg/L NH₂OH-N). [Color figure can be seen in the online version of this article, available at www.interscience.wiley.com.]

(2) reduction of mass transfer resistance because of physical changes in the aggregate structure.

In our study, addition of NH₂OH to autotrophic nitrifying cultures in 6-h batch experiments enhanced initial NH₃-N uptake rates by a factor of 1.4–13. The primary mechanism for this effect was likely physiological stimulation because the enhanced NH₃-N removal rate coincided with the rapid uptake of NH₂OH. This only applies to the short term effect of NH₂OH addition, because the enhancement of NH₃-N uptake rate occurred only when NH₂OH was available and not when NH₂OH had been depleted. The second hypothesis focuses on floc disaggregation. In the current

work, NH₂OH addition in 6-h batch experiments changed the physical structure of the nitrifying aggregates. NH₂OH addition caused a 20–40% decrease in the median aggregate size and broadened the shape of the aggregate size distribution by up to 230%. NH₂OH addition caused some of the AOB microcolonies to appear more dispersed. The aggregate size shift was rarely observed as a reduction in all aggregate sizes (as in disaggregation), but instead, it was more commonly observed as a broadening of the size distribution and a reduction of the median aggregate size. This “broadening” of the size distribution probably played no role in accelerating NH₃-N uptake kinetics because the rate enhancement was not sustained throughout the 6-h experi-

ment; it was only present initially (when NH_2OH was also present). Actually, neither of the two hypotheses seems to hold for longer term effects of NH_2OH addition on nitrification because the overall effects were inhibitory. The short term benefits of NH_2OH addition were eventually outweighed by longer term inhibition.

There may be a reactive chemical species capable of causing the inhibition and structural changes documented in the current work. One possible explanation for NH_2OH -induced effects is hydrogen peroxide, generated by the reduction of oxygen by NH_2OH (Choudhary and Jana, 2008):



Peroxide is a highly reactive byproduct capable for oxidizing inert material and active biomass. Choudhary and Jana (2008) and Song et al. (2008) abiotically produced hydrogen peroxide in the presence of suitable catalysts like trace metals or quinone/semiquinone-like structures. The autooxidation of NH_2OH may have taken place in the bioreactors used in the current study because of the catalytic properties of metal ions supplied to the bioreactors as part of the medium and oxygen containing quinone/semiquinone-like structures that are commonly found on the surface of the cell wall (Madigan et al., 1997).

Choudhary and Jana (2008) found that H_2O_2 can react with NH_2OH producing water and nitrogen gas:



This means that NH_2OH may mediate both the generation and degradation of H_2O_2 , and therefore, high concentrations of NH_2OH can scavenge H_2O_2 . This “self-inhibitory” effect of NH_2OH on H_2O_2 production would be consistent with the fact that, in the current FBBR work, the strongest negative responses were observed at 20 mg NH_2OH -N/L and not at 40 mg NH_2OH -N/L.

This peroxide hypothesis was investigated in batch experiments, and H_2O_2 was measured by the potassium permanganate titration, but this method was not sensitive enough to detect H_2O_2 in the samples or in prepared standards of 5 mg H_2O_2 /L or less. Thus, these preliminary experiments were inconclusive. Future experiments should employ more sensitive methods for detecting H_2O_2 production in nitrifying cultures exposed to NH_2OH .

This research expands what is currently known about the effect of NH_2OH on nitrifying systems. First, it shows that NH_2OH addition can act as an enhancer (on the short term) and an inhibitor (on a longer term) of ammonia uptake rates. The previous reports (e.g., Hyman and Wood, 1983; Kindaichi et al., 2004a; Kuai and Verstraete, 1998; Yang and Alleman, 1992) only reported either one of these aspects, which presented an apparent conflict. Second, the current work shows that NH_2OH addition can lead to inhibition of AOB, not just NOB (as suggested by Kindaichi et al., 2004a). The implication of this is that increasing NH_2OH concentration is not a good strategy to favor AOB over NOB. Third, this work shows that the longer term effect of NH_2OH concentration on nitrifying aggregates is

complex and nonlinear, because the negative effects appear attenuated and/or delayed at higher NH_2OH levels. Finally, the current work shows that NH_2OH addition causes the floc structures to change (and become more dispersed) at the micro and macro level.

This research impacts the study of nitrification, and it shows that NH_2OH should be monitored in bench and pilot scale experiments. This is particularly relevant for simultaneous nitrification/denitrification systems (SND) (i.e., systems that nitrify and denitrify via nitrite), because these systems periodically accumulate NH_2OH (Yang and Alleman, 1992). Occasional build up of small amounts of NH_2OH may enhance NH_3 uptake, but consistent NH_2OH accumulation is likely to inhibit nitrification. These NH_2OH dynamics may have a significant impact on SND systems. Thus, SND models should be empirically revised to capture the potential of NH_2OH -related enhancement or inhibition of the nitrifying biomass. Also, because nitrifiers are known to become inhibited by several factors, the study of nitrification in engineered and natural systems should include close attention to NH_2OH dynamics in order to avoid misinterpretations.

Conclusion

Addition of hydroxylamine (NH_2OH) to autotrophic nitrifying cultures in 6-h batch experiments enhanced initial NH_3 -N uptake rates by a factor of 1.4–13. The primary mechanism for this effect is physiological stimulation because the enhanced NH_3 -N removal rate coincided with the rapid uptake of NH_2OH . NH_2OH addition in 6-h batch experiments changed the physical structure of the nitrifying aggregates. NH_2OH addition caused a 20–40% decrease in the median aggregate size and broadened the shape of the aggregate size distribution by up to 230%. NH_2OH addition caused some of the AOB microcolonies to appear more dispersed. Longer term NH_2OH addition in fed batch bioreactors (FBBRs) shifted the aggregate size distribution, and eventually caused NH_3 -N removal to decrease from >90 to 75–17%. The deterioration in FBBR performance was explained by quantitative FISH results that show inhibition of NOB and AOB populations, and by qPCR results showing that the copy numbers of *amoA* and *nxrA* genes gradually decreased by up to an order-of-magnitude.

The authors thank Mette Larsen (Technical University of Denmark, Chemical Engineering Department) for conducting aggregate size analysis, Claire Commeaux (INRA, CNRS, Université de Lyon) for guidance of qPCR for *nxrA*, and Taewoo Yi (University of Pittsburgh, Civil and Environmental Engineering) for experimental assistance. The authors thank the Danish Agency for Science Technology and Innovation (FTP-ReSCoBiR) and the National Science Foundation (via International Research and Education in Engineering program, BES award no. 0546388) for financial support. The authors also thank the anonymous reviewers for their suggestions.

References

- Alm EW, Oerther DB, Larsen N, Stahl DA, Raskin L. 1996. The oligonucleotide probe database. *Appl Environ Microbiol* 62:3557–3559.
- Amann RI, Binder BJ, Olson RJ, Chisholm SW, Devereux R, Stahl DA. 1990. Combination of 16S rRNA-targeted oligonucleotide probes with flow cytometry for analyzing mixed microbial populations. *Appl Environ Microbiol* 56:1919–1925.
- Amann RI. 1995. In situ identification of microorganisms by whole cell hybridization with rRNA-targeted nucleic acid probes. In: Akkeman ADC, van Elsas JD, de Bruijn FJ, editors. *Molecular microbial ecology manual*. Dordrecht: Kluwer Academic.
- APHA. 1992. *Standard Methods for the Examination of Water and Wastewater*. Washington D.C.: American Public Health Association.
- Blackburne R, Carvalho G, Yuan ZG, Keller J. 2003. Selective production of nitrite using hydroxylamine as inhibitor of nitrite oxidation. Kuala Lumpur, Malaysia: International Water Association. p 186–193.
- Böttcher B, Koops H. 1994. Growth of lithotrophic ammonia-oxidizing bacteria on hydroxylamine. *FEMS Microbiol Lett* 122:263–266.
- Chandran K, Smets BF. 2008. Biokinetic characterization of the acceleration phase in autotrophic ammonia oxidation. *Water Environ Res* 80(8):732–739.
- Choudhary V, Jana P. 2008. Factors influencing the in situ generation of hydrogen peroxide from the reduction of oxygen by hydroxylamine from hydroxylammonium sulfate over Pd/alumina. *Appl Catal A* 335:95–102.
- Daims H, Bruhl A, Amann RI, Schleifer KH, Wagner M. 1999. The domain-specific probe EUB338 is insufficient for the detection of all Bacteria: Development and evaluation of a more comprehensive probe set. *Syst Appl Microbiol* 22:434–444.
- Daims H, Nielsen JL, Nielsen PH, Schliefer KH, Wagner M. 2001. In situ characterization of Nitrospira-like nitrite-oxidizing bacteria active in wastewater treatment plants. *Appl Environ Microbiol* 67:5273–5284.
- Daims H, Lucker S, Wagner M. 2006. Daime, a novel image analysis program for microbial ecology and biofilm research. *Environ Microbiol* 8:200–213.
- de Bruijn P, van de Graaf A, Jetten M, Robertson L, Kuenen J. 1995. Growth of *Nitrosomonas europaea* on hydroxylamine. *FEMS Microbiol Lett* 125:179–184.
- Dua RD, Bhandari B, Nicholas DJD. 1979. Stable isotope studies on the oxidation of ammonia to hydroxylamine by *Nitrosomonas europaea*. *FEBS Lett* 106(2):401–404.
- Frear DS, Burrell RC. 1955. Spectrophotometric method for determining hydroxylamine reductase activity in higher plants. *Anal Chem* 27:1664–1665.
- Hyman M, Wood P. 1983. Methane oxidation by *Nitrosomonas europaea*. *Appl Environ Microbiol* 212:31–37.
- Iizumi T, Mizumoto M, Nakamura K. 1998. A bioluminescence assay using *Nitrosomonas europaea* for rapid and sensitive detection of nitrification inhibitors. *Appl Environ Microbiol* 64:3656–3662.
- Kindaichi T, Okabe S, Satoh H, Watanabe Y. 2004a. Effects of hydroxylamine on microbial community structure and function of autotrophic nitrifying biofilms determined by in situ hybridization and the use of microelectrodes. *Water Sci Technol* 49:61–68.
- Kindaichi T, Ito T, Okabe S. 2004b. Ecophysiological interaction between nitrifying bacteria and heterotrophic bacteria in autotrophic nitrifying biofilms as determined by microautoradiography-fluorescence in situ hybridization. *Appl Environ Microbiol* 70:1641–1650.
- Kuai L, Verstraete W. 1998. Ammonium removal by the oxygen-limited autotrophic nitrification-denitrification system. *Appl Environ Microbiol* 64:4500–4506.
- Lydmark P, Lind M, Sörensson F, Hermansson M. 2006. Vertical distribution of nitrifying populations in bacterial biofilms from a full-scale nitrifying trickling filter. *Environ Microbiol* 8:2036–2049.
- Madigan MT, Martinko JM, Parker J. 1997. *Brock biology of microorganisms*. Upper Saddle River, NJ: Prentice-Hall.
- Mobarry BK, Wagner M, Urbain V, Rittmann BE, Stahl DA. 1996. Phylogenetic probes for analyzing abundance and spatial organization of nitrifying bacteria. *Appl Environ Microbiol* 62:2156–2162.
- Poly F, Wertz S, Brothier E, Degrange V. 2008. First exploration of *Nitrobacter* diversity in soils by a PCR cloning-sequencing approach targeting functional gene *nxrA*. *FEMS Microbiol Ecol* 63:132–140.
- Pynaert K, Smets BF, Wyffels S, Beheydt D, Siciliano SD, Verstraete W. 2003. Characterization of an autotrophic nitrogen-removing biofilm from a highly loaded lab-scale rotating biological contactor. *Appl Environ Microbiol* 69:3626–3635.
- Rittmann BE, Snoeyink VL. 1984. Achieving biologically stable drinking water. *J Am Water Works Assoc* 76:106–114.
- Rotthauwe JH, Witzel KP, Liesack W. 1997. The ammonia monooxygenase structural gene *amoA* as a functional marker: Molecular fine-scale analysis of natural ammonia-oxidizing populations. *Appl Environ Microbiol* 63:4704–4712.
- Schmidt I, Look C, Bock E, Jetten MSM. 2004. Ammonium and hydroxylamine uptake and accumulation in *Nitrosomonas*. *Microbiol* 150:1405–1412.
- Song W, Li J, Liu J, Shen W. 2008. Production of hydrogen peroxide by the reaction of hydroxylamine and molecular oxygen over activated carbons. *Catal Commun* 9:831–836.
- Wagner M, Rath G, Koops HP, Flood J, Amann R. 1996. In situ analysis of nitrifying bacteria in sewage treatment plants. *Water Sci Technol* 34:237–244.
- Wallner G, Amann R, Beisker W. 1993. Optimizing fluorescent in situ hybridization with rRNA-targeted oligonucleotide probes for flow cytometric identification of microorganisms. *Cytometry* 14:136–143.
- Watson S, Brock E, Harms H, Koops H. 1984. Ammonia oxidizing bacteria. In: Williams ST, Sharpe ME, Holt JG, editors. *Bergey's Manual of Systematic Bacteriology*, Vol. 3. New York: Springer. p 1808–1834.
- Wertz S, Poly F, Le Roux X. 2008. Development and application of a PCR-denaturing gradient gel electrophoresis tool to study the diversity of *Nitrobacter*-like *nxrA* sequences in soil. *Fems Microbiol Ecol* 63:261–271.
- Yang L, Alleman JE. 1992. Investigation of batch-wise nitrite build-up by an enriched nitrification culture. *Water Sci Technol* 26:997–1005.